Applying DTI white matter orientations to finite element head models to examine diffuse TBI under high rotational accelerations

Niall C. Colgan[a,b,], Michael D. Gilchrist[b,c], Kathleen M. Curran[*,a]

[a] *Diagnostic Imaging, University College Dublin, Belfield, D4, Ireland*
[b] *Mechanical Engineering, University College Dublin, Belfield, D4, Ireland*
[c] *School of Human Kinetics, University of Ottawa, Ontario K1N 6N5, Canada*

Abstract

The in-vivo mechanical response of neural tissue during impact loading of the head is simulated using geometrically accurate finite element (FE) head models. However current FE models do not account for the anisotropic elastic material behaviour of brain tissue. In soft biological tissue, there is a correlation between internal microscopic structure and macroscopic mechanical properties. Therefore, constitutive equations are important for the numerical analysis of the soft biological tissues. By exploiting diffusion tensor techniques the anisotropic orientation of neural tissue is incorporated into a non-linear viscoelastic material model for brain tissue and implemented in an explicit FE analysis. The viscoelastic material parameters are derived from published data and the viscoelastic model is used to describe the mechanical response of brain tissue. The model is formulated in terms of a large strain viscoelastic framework and considers non-linear viscous deformations in combination with non-linear elastic behaviour. The constitutive model was applied in the University College Dublin brain trauma model (UCDBTM) (i.e. three-dimensional finite element head model) to predict the mechanical response of the intra-cranial contents due to rotational injury.

Key words: Nonlinear elasticity, Anisotropy, Impact biomechanics, Traumatic brain injury

[*]Corresponding author
Email address: Kathleen.Curran@ucd.ie (Kathleen M. Curran)

1. Introduction

Nearly two million traumatic brain injuries (TBIs) occur annually in the United States and it is the leading cause of death and disability in 15-24 year-olds (Langlois et al., 2004, Sorenson and Kraus, 1991). TBI also accounts for one million hospital admissions annually in the European Union (Bowen et al., 1997). The past two decades have seen a large increase in the use of computational biomechanical models as investigative tools in head injury research (Johnson and Young, 2005; Muller and Ruegsegger, 1995; Ruan et al., 1991, 1994, 1993; Kleiven, 2002; Kleiven and Holst, 2002; Horgan and Gilchrist, 2003, 2004; Miller and Chinzei, 1997). These models use either finite element methods or multi-body dynamic simulations to suggest the tolerance levels for the occurrence of head injury using various measured mechanical parameters and the probability of specific head injury sequelae that are associated with TBI (Auer et al., 2001; Doorly and Gilchrist, 2006; Baumgartner et al., 2001; Willinger and Baumgartner, 2003).

Diffuse white matter damage is associated with a large fraction of those patients with poor neurological outcome in adult and paediatric survivors of brain injury, ranging from subtle behavioural changes to significant neurological deficits (Colgan et al., 2010). Biomechanical analyses of high rotational acceleration/deceleration associated with diffuse axonal injury (DAI) suggest a link between brain material response (strain) and the orientation of the associated injured white matter (Halabieh and Wan, 2008; Parizel et al., 1998).

Neuronal/axonal injury has been implicated as the leading pathologic lesion of TBI, with secondary damage resulting from numerous neurodegenerative cascades (Smith and Meaney, 2000). Traumatic axonal injury, attributed to shear and tensile stresses, typically occurs in the white matter of the cerebral hemispheres, corpus callosum, and brain stem, especially in severe TBI (Hurley et al., 2004). Diffuse axonal injury, associated with high rotational acceleration/deceleration, often results in apoptosis at sites distal to the centre of rotation of the head (Conti et al., 1998; Holmin et al., 1998; Williams et al., 2006).

Based on the involvement of complex neurocognitive pathways of varying orientations, we hypothesise that the predicted severity and location of the sites of injury are influenced by the orientation of the neuronal fibres in the reference frame of the applied global forces in the FE simulation. The objective of this study is to establish the orientation of the neural fibres

within the brain using diffusion tensor imaging and apply these orientations into the 3D UCDBTM FE model (Horgan and Gilchrist, 2003, 2004) to assess the effects of anisotropy on simulated results of a high rotational TBI.

2. Materials and methods

The method used to define the orientation of the fibres within the brain is magnet resonance diffusion tensor imaging (DTI). Diffusion Tensor Imaging (Basser et al., 1994) is an MRI technique that measures the diffusion orientation of water in tissue. Using the measured diffusion of water within highly directional tissue, for example neuronal white matter, it is possible to extract information relating to the trajectory of axonal fibres within the brain. DTI essentially provides two distinct sets of information based on the Brownian motion of water in the specific tissue being scanned;

1. anisotropy of the diffusion (e.g. fractional anisotropy (FA))
2. direction in which the diffusion is occurring

By assuming that the largest principal axis of the diffusion tensor aligns with the predominant fibre orientation in an MRI voxel, we can obtain 2D or 3D vector fields that represent the fibre orientation at each voxel. The 3D reconstruction of tract trajectories, or tractography, is a natural extension of such vector fields. This is the simplest method of tract generation and is used in this current study, however this method can be prone to error.

The normalised DTI volume used is an example file from Fiber Viewer (Goodlett et al., 2005). The image set voxel size of 2x2x2 mm isotropic and the averaged diffusion vector of the water molecules contained in each voxel is based on six principal diffusion direction gradients. The voxel size is small enough to distinguish white and grey matter (Figure 1 A). The white matter consists of tracts that run along various directions and are large enough to discern visually (Figure 1 A and B). The image resolution is sufficiently high for the white matter tracts to span several voxels. The white matter tracts, in turn, consist of densely packed axons (neuronal projections) in addition to various types of neuroglia and other small populations of cells. Inside the voxel, water molecules are distributed between these cell types and the extracellular space (80–85% are intracellular). Assuming that the orientation of the largest component of the diffusion tensor represents the orientation of dominant axonal tracts, DTI can provide a 3D vector field, in which each vector represents the fibre orientation denoted by λ (Figure 1 C and Figure

2). Currently, there are several different approaches to reconstruct white

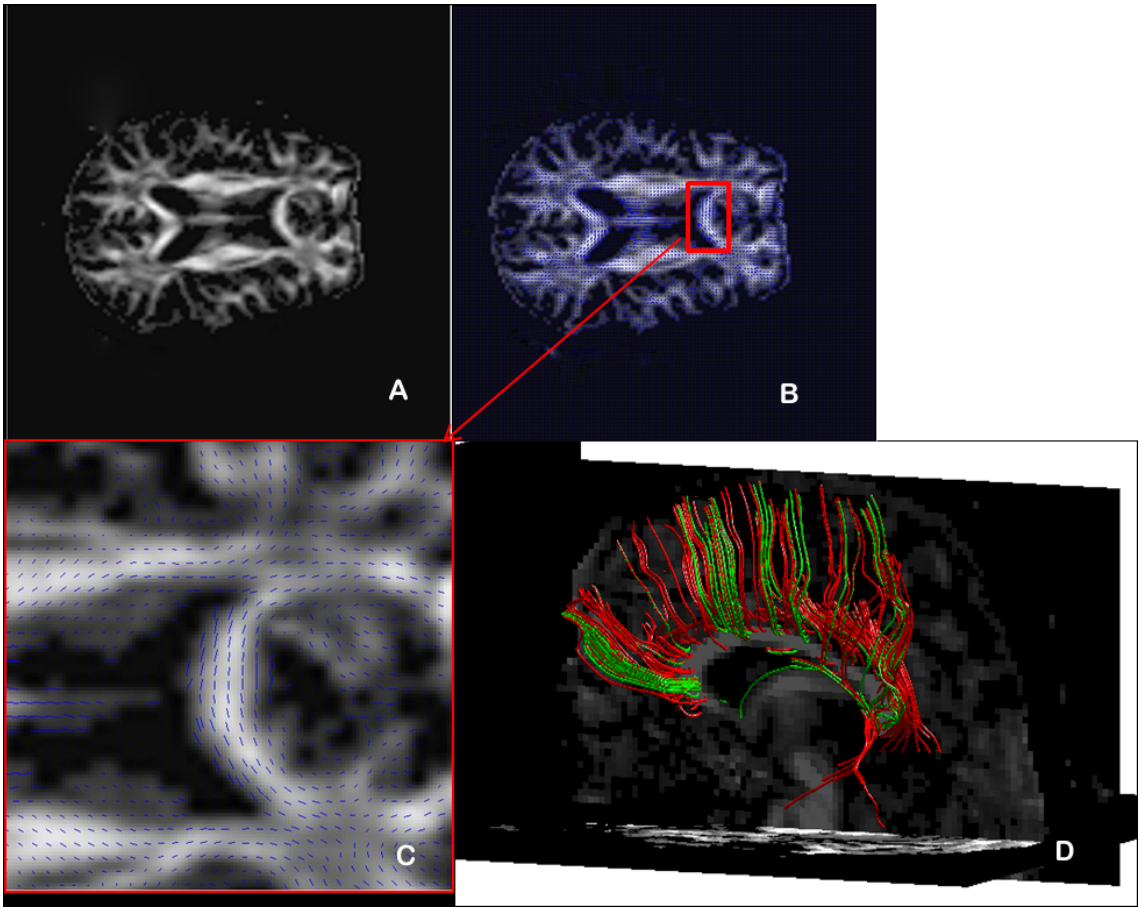

Figure 1: Typical DTI volume (taken from Fiber ViewerGoodlett et al, 2005) (A) FA map of the mid-transverse slice of the human head (B) FA map overlaid with the vectormap of the diffusion tensor (C) Zoomed view of the anterior corpus callosum outlined in B showing the 2D vector orientations (D) The 3D axonal tract representation of the corpus callosum and the corona radiata.

matter tract representations, which can be broadly classified into two types: deterministic and probabilistic. Techniques classified in the first category are based on line propagation algorithms that use local tensor information for each step of the propagation. The main differences among techniques stems from the way information from neighbouring pixels is incorporated to define smooth trajectories or to minimize noise contributions. The second type of

approach is based on global energy minimization to find the energetically most favourable path between two predetermined pixels. The most intuitive way to reconstruct a 3D trajectory from a 3D vector field is to propagate a line from a seed point by following the local vector orientation (Figure 1D) where the mean diffusivity is represented by λ' which is generated from the principal eigenvalues (λ_1, λ_2, λ_3) by the equation

$$\lambda' = (\lambda_1 + \lambda_2 + \lambda_3)/3 \tag{1}$$

The FA index measures the fraction of the magnitude of the effective diffusion tensor that is ascribed to the anisotropic diffusion. FA is is quantitative and dimensionless. For an isotropic medium, FA = 0 and for a cylindrically symmetric anisotropic medium (i.e., $\lambda_1 > \lambda_2$, $\lambda_2 = \lambda_3$), FA =1 (Basser and Pierpaoli, 1996). The anisotropy (FA) of the voxel containing the diffusion tensor is generated by the equation

$$FA = \sqrt{\frac{1}{2}} \frac{\sqrt{(\lambda_1 - \lambda_2)^2 + (\lambda_1 - \lambda_3)^2 + (\lambda_2 - \lambda_3)^2}}{\sqrt{((\lambda_1)^2 + (\lambda_2)^2 + (\lambda_3)^2)}} \tag{2}$$

The linear propagation approach, which was dubbed FACT (fibre assignment by continuous tracking) (Mori et al., 1999), was used to reconstruct the tract trajectories. The vector information contained at each voxel may not fully reflect the propagation of all the neurons within each voxel but instead it reflects the principal orientation of the fibres within each voxel. This is due to the resolution capabilities of the MRI. The average central nervous system axon is approximately $1\mu m$ in diameter and the voxel size in this study is 2x2x2 mm and regions where fibres cross maybe represented as isotropic (eq. 2) but may in fact, contain two distinct tensor propagations (Tuch et al., 2002). However, the tensor information that is used in the FE model is fitted to the elements with an approximate size of $10mm^3$ and the distinct tensors that define each voxel region are again averaged to give the gross representation of the fibre orientations of each element in the UCDBTM head model.

2.1. Mesh morphing to apply orientations

The location and orientation of the tensor information and the FA is mapped to each element by registering the elements that comprise the brain in the 3D FE model to the 3D FA volume of the brain. Registration of DT images requires optimisation of tensor reorientation (Alexander et al, 2001;

Curran and Alexander, 2003, 2004; Zhang et al, 2006). However, the FE elements were mapped to the FA volume negating the requirement for tensor reorientation. Creation of another subject specific FE model of the entire head was considered to be beyond the scope of this present work. Instead the existing validated model was morphed to the 3D MR volume using a thin-plate splines method to compute the full-field transformations between source (FE model) and target (FA volume). This has the basis that a plate with isotropic properties (eg. steel) can be morphed to fit a homologous shape (a shape that can be formed from the original without joining, crossing or tearing the original shape) by means of applying forces and constraints to bend the plate to the new desired shape. Instead of writing a program to perform this morphing, a combination of Matlab subroutines and ABAQUS software was used instead to reshape the model. A coarse surface grid mesh of the brain FE model was constructed and this was then warped (simple scaling in the X, Y and Z domains) to fit the global x, y and z dimensions of 3D FA Volume (Mendis et al., 1995).

Vectors were constructed by using the node points on the coarse grid and matching landmark points based on the shortest distace from the node grid positions to the surface of the FA volume, until every point on the coarse grid had a displacement vector associated with it. A static displacement analysis, using all of these displacement vectors as input, was then carried out on this coarse grid (giving it isotropic properties). Using Matlab the resultant vector plot was transformed into a continuous spatial displacement field. This new continuous displacement field was then applied to the projection mesh model at the dura and a new static displacement analysis was carried out on the entire projection mesh model (again giving all elements identical isotropic properties). This then forced the intracranial shape to move from its original state to match that of the new intracranial shape. Finally the analysis results were used to create an applied spatial transformation in Matlab which moved the original nodal positions, strain free, to those of the deformed positions. This process was used to find the principle orientation of each element in the original FE space; the anisotropy from DTI was then integrated with the model (Figure 2 A and B).

2.2. Material model

A constitutive model with transversely isotropic hyperelastic mechanical behaviour of a family of collagen fibres for the arterial wall has been developed Gasser et al.,(2006) and Holzapfel et al.,(2000). Therefore, this model

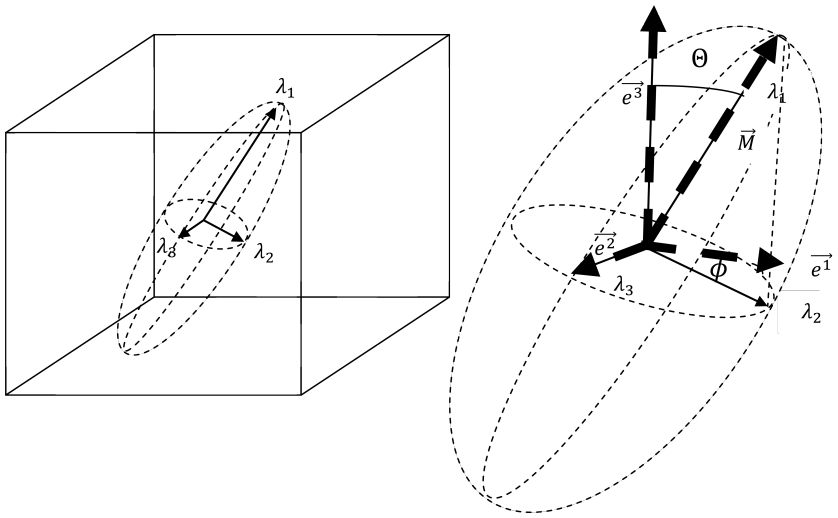

Figure 2: A 3D eigenvetor representation of the diffusion direction and arbitrary unit direction vector $\overrightarrow{M}$ in terms of Eulerian angles

provides a good bases from which to develop a similar hyperelastic model for anisotropic regions of brain tissue. It is assumed that there is only one family of axonal fibre bundles and these axonal fibres are embedded in an isotropic incompressible matrix. These axonal fibres are distributed uniaxially in an inferior-superior direction. For the purpose of simplification, the preferred fibre direction vector, $\overrightarrow{n_0}$, is aligned within a local rectangular cartesian coordinate system and the orientation density function is independent of Eulerian angle, Φ, as defined in the DTI tensor. Therefore, the orientation density function, $\rho(\overrightarrow{M}(\Theta,\Phi))$, becomes $\rho(\overrightarrow{M}(\Theta))$.

$$\alpha_{11} = \alpha_{22} = k, \alpha_{33} = 1 - 2k, k = \frac{1}{4}\int_0^{\pi} \rho\left(\vec{M}(\Theta)\right) sin^3\Theta d\Theta \tag{3}$$

where the term k has been introduced to represent the fibre distribution and describes the degree of anisotropy. Consequently, the generalized second order structure tensor, H, can be written in compact form.

$$H = kI + (1 - 3k)\vec{n_0}\vec{n_0} \tag{4}$$

where I is the identity tensor. Hence, H depends only on the single dispersion structural parameter k ($k \in [0,\ 1/3]$).k=0 describes the full alignment of axonal fibres and $k = 1/3$ describes the isotropic distribution of axonal fibres. The continuum representation of the axonal fibre orientation forms the foundation for an anisotropic hyperelastic formulation. In order to derive the anisotropic hyperelastic strain energy potential W for the brain, it is assumed that it can be separated into an isotropic strain energy potential of the matrix, W_m and an anisotropic strain energy potential of axonal fibers, W_f. Therefore, the anisotropic strain energy potential function is

$$W\left(\bar{C}, H_i\right) = W_m\left(\bar{C}\right) + \sum_{i=1}^{N} W_{fi}\left(\bar{C}, H_i(\vec{n_o}i, k)\right) \tag{5}$$

where the general second order structural tensor $H_i\left(\overrightarrow{n_{oi}},\ k\right)$ is defined according to equation (4), N is the number of fibre families and $\overline{C}$ is the isochoric part of the right Cauchy-Green strain tensor C.

The matrix material is modelled as an incompressible isotropic neo-Hookean model (Ning et al., 2006, Hrapko et al., 2008, Van Dommelen et al., 2008, Prange and Margulies, 2002), i.e.

$$W_m = C_{10}\left(\overline{I_1} - 3\right) + \frac{1}{D_1}(J-1)^2 \tag{6}$$

where $\overline{I_1}$ denotes the first invariant of $\overline{C}$, J is the volume ratio, C_{10} and D_1 are neo-Hookean coefficients. These neo-Hookean coefficients can be related to the initial shear modulus G_0 and the bulk modulus K_0 as follows

$$C_{10} = \frac{G_0}{2}, D_1 = \frac{2}{K_0} \tag{7}$$

The additional contribution of the anisotropic strain energy potential for the ith family of axonal fibres is

$$W_{fi}\left(\bar{C}, H_i\right) = \frac{k_1}{2k_2}\sum_{i=1}^{N}\left(e^{k_2\bar{E}_1^2} - 1\right) \tag{8}$$

where $k_1 > 0$ is a stress parameter to quantify mechanical tensile strength of the axonal fibres and $k_2 > 0$ is a dimensionless parameter. The important fundamental hypothesis of the Holzapfel-Gasser-Ogden model (Abaqus, 2007) is that the axonal fibres cannot support any compression and would buckle

under compressive load, i.e, fibres contribute only their mechanical strength during tension. The strain energy potential function of the isotropic matrix and the contribution from the anisotropic axonal fibre reinforcements is given by

$$W = C_{10}\left(\bar{I}_1 - 3\right) + \frac{1}{D_1}\left(\frac{J^2-1}{2} - lnJ\right) + \frac{k_1}{2k_2}\sum_{i=1}^{N}\left(e^{k_2\langle\bar{E}_i\rangle^2} - 1\right) \qquad (9)$$

This Holzapfel-Gasser-Ogden material definition was used to model the white matter tracts using the direction dependant material properties in the literature (Arbogast and Margulies, 1999; Prange and Margulies, 2002; Ning et al., 2006), as summarised in Table 1.

Brain	G_0	C_{10}	K_0	D_1	k_1	k_2	k
	[Pa]	[Pa]	[GPa]	[1/GPa]	[Pa]		
Brain	315.17	157.88	2	1	3013.30	0.00001	FA
Brainstem	12.7	6.35	2	1	121.2	01	FA

Table 1: Material properties of the brain

The dispersion parameter k is defined based on the average fractional anisotropy equation (2) of the fibres for each element group. The material properties of the brain stem are highly anisotropic in nature and are defined separately to the remaining brain tissue that constitute the elements of the cerebrum. The material properties for the remaining parts of the model, i.e., the cortical and trabecular bone, scalp and intracranial membranes were taken from the literature (Horgan and Gilchrist, 2003).

The UCDBTM, which is a freely available, validated 3D finite element model of the head, can simulate the effect of the overall head movement on the cranial contents, so the local deformation parameters within the brain tissue can be examined and compared to the observed clinical results. The analysis of the model boundary conditions and mesh sensitivity have been previously assessed (Horgan and Gilchrist, 2003, 2004) while validating the model against linear and rotational impact cadaver tests.

An experimental study of high rotational acceleration/deceleration on monkeys (Gennarelli et al., 1982) reported the conditions required to produce diffuse axonal injury (DAI). At levels of acceleration below 175 $krad/s^2$

Material	Young's modulus (MPA)	Poisson's ratio	Density (kg/m3)
scalp	16.7	0.42	1000
Cortical bone	15000	0.22	2000
Trabecular bone	1000	0.24	1300
Dura	31.5	0.45	1130
Pia	11.5	0.45	1130
Falx and Tentorium	31.5	0.45	1130
Facial Bone	5000	0.23	2100

Table 2: Material properties of the remaining head structures

and pulse duration below 5ms cerebral concussion was present and it was proposed that a shear strain of 0.05 was necessary to cause concussion (Margulies and Thibault, 1994). This rotational acceleration was applied in the sagittal plane around the centre of mass of the present 3D model with both the anisotropic material properties (i.e., $k = 0$) and isotropic material properties (i.e., $k = 1/3$) from the literature (Table 1). Elements were segmented manually and grouped together to represent specifc structures and regions based on the segmented fibre bundle representations in the DTI data set. The gross orientations were overlaid onto the FE head model.

3. Results

The predicted regions affected by axonal injury were based on the shear strain response of each material model and the results of which are presented in Figure 3. The model predicted a statistically significant difference between homogenous and anisotropic material definitions at both the brainstem and the corona radiata ($p<0.05$) regions. However, within the midbrain, corpus callosum and grey matter regions, no significant difference was predicted by using either isotropic or anisotropic properties.

These two regions where differences were observed are highly anisotropic with a median fractional anisotropy (FA) value of 0.7 with a standard deviation of 0.003. The grey matter however does not have a principle orientation

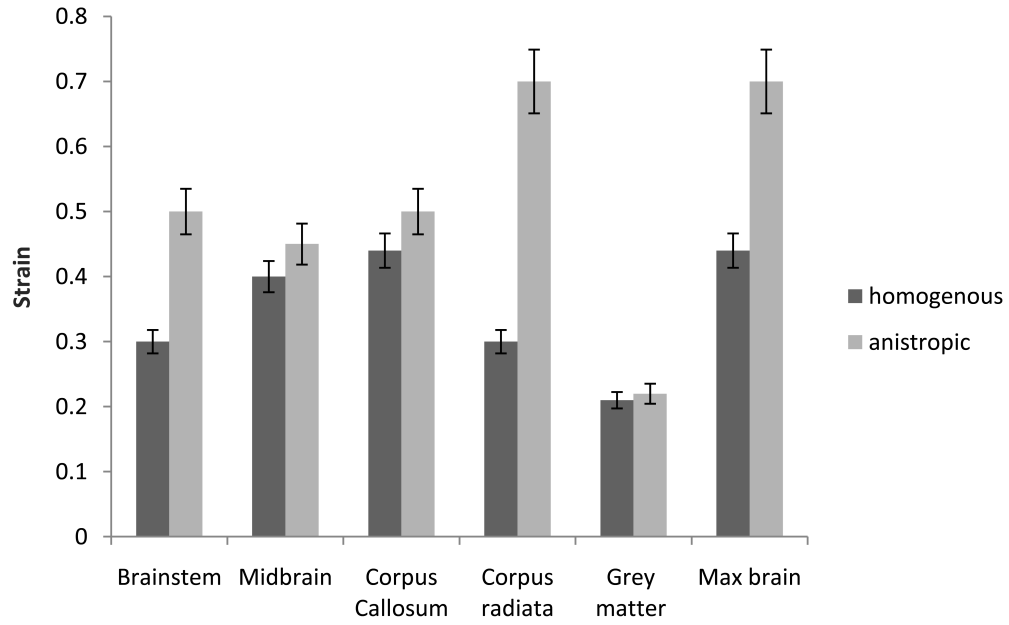

Figure 3: The mean values and standard deviations observed in the simulations for strain based measures

and has a max FA of less than 0.1. No statistically significant difference was found between the shear strain of the anisotropic grey matter and the homogenous grey matter ($p<0.01$). Similarly too, no statistically significant difference in axonal injury was predicted between the material models for the Corpus Callosum and the Midbrain. These regions have FA values of 0.8 and 0.7 respectively and are highly anisotropic and a larger variation between the material responses was expected. This may be due to the location of the centre of mass around which the rotation takes place and the principle orientations of the white matter in these regions lie along the axis of rotation. This would result in a reduction in the shear forces acting in these fibres.

4. Discussion

In current research, finite element modelling is the primary tool used to investigate the mechanics of TBI. However the material models are crucial in accurately predicting the circumstances that cause TBI. The approach of

combining in-vivo measurements of the orientations of normal healthy axonal fibre bundles with FE models could improve the predictive capabilities using FE simulations in DAI. The current practice of using homogenous material properties may lead to erroneous results in the reported values of injury in numerical accident reconstruction. The initial quality of the elements in the present model was assessed and confirmed to be adequate and the total energy remained constant while the hourglassing energy was insignificant compared to the total energy in the calculations (<10%). However, one possible limitation of the present model is the relatively low mesh density of the head model in comparison to the DTI data. This limits the geometrical detail that would be required to model each individual axonal tract, especially the interface between grey and white matter tracts and the boundaries of the ventricular system and white matter. Another limitation of the model is the orientation of the tensors within each element. The registration method may not fully map each voxel to its exact location within each element and the method of generating the tracts could also lead to errors in the ellipsoid placement. However subject specific models with a mesh density of $1mm^3$ along with higher order tensor data and noise reduction methods would improve the FE predictions but would also increase the computation time of each simulation.

5. Conclusion

The FE model predictions illustrate the importance of the orientation of the material structure in diffuse axonal injury. The anisotropic model predicted a greater level of injury at sites distal to the centre of rotation than a simple isotropic model. These findings illustrate that the anisotropic model shows a varation in the predicted apoptosis at sites distal to the centre of rotation in diffuse axonal injury simulation.

ABAQUS, version 6.9-2, (2007) ABAQUS analysis: user's manual, Dassault systemes.
ALEXANDER, D.C., PIERPAOLI, C., BASSER P.J., GEE J.C. (2001) Spatial transformations of diffusion tensor magnetic resonance images. IEEE transactions in medical imaging. 20, 1131-1139.
AUER, C., SCHONPFLUG, M. & BEIER, G. (2001) An analysis of brain injuries in real world pedestrian traffic accidents by computer simulation reconstruction. Proceedings of the International Society of Biomechanics XVIIIth Congress.
BASSER, P. J., MATTIELLO, J. & LEBIHAN, D. (1994) MR diffusion tensor spectroscopy and imaging. Biophysical Journal, 66, 259-267.
BASSER, P. J. & PIERPAOLI, C. (1996) Microstructural and physiological features of tissues elucidated by quantitative-diffusion-tensor MRI. Journal of Magnetic Resonance, Series B, 111, 209-219.
BAUMGARTNER, D., WILLINGER, R., SHEWCHENKO, N. & BEUSENBERG, M. (2001) Tolerance limits for mild traumatic brain injury derived from numerical head impact replication. Proceedings of the 2001 International IRCOBI Conference on the Biomechanics of Impacts, 353-355.
BOWEN, J. M., CLARK, E., BIGLER, E. D., GARDNER, M., NILSSON, D., GOOCH, J. & POMPA, J. (1997) Childhood traumatic brain injury: neuropsychological status at the time of hospital discharge. Developmental Medicine and Child Neurology, 39, 17-25.
COLGAN, N.C., CRONIN, M.M., GOBBO, O.L., OMARA, S.M., OCONNOR, W.T. & GILCHRIST, M.D. (2010) Quantitative MRI analysis of the experimental evolution of mild and severe TBI. Journal of Neurotrauma, 27(7): 1265-1274
CONTI, A. C., RAGHUPATHI, R., TROJANOWSKI, J. Q. & MCINTOSH, T. K. (1998) Experimental brain injury induces regionally distinct apoptosis during the acute and delayed post-traumatic period. Journal of Neuroscience, 18, 56-63.
CURRAN, K. M. & ALEXANDER, D. C. (2003) Diffusion tensor orientation matching for image registration. Proceedings of SPIE International Society for Optical Engineering. Medical Imaging 2003: Image Processing; 5032: 149-156.
CURRAN, K. M. & ALEXANDER, D. C. (2004) Orientation coherence optimisation in tensor image registration, Proceedings of the 13th International Society for Magnetic Resonance in Medicine.
DOORLY, M. C. & GILCHRIST, M. D. (2006) The use of accident recon-

struction for the analysis of traumatic brain injury due to head impacts arising from falls. Computer Methods in Biomechanics and Biomedical Engineering, 9, 371-377.
GASSER, T. C., OGDEN, R. W. & HOLZAPFEL, G. A. (2006) Hyperelastic modelling of arterial layers with distributed collagen fibre orientations. Journal of the Royal Society Interface, 6, 15-35 .
GENNARELLI, T. A., THIBAULT, L. E., ADAMS, J. H., GRAHAM, D. I., THOMPSON, C. J. & MARCINCIN, R. P. (1982) Diffuse axonal injury and traumatic coma in the primate. Annals of Neurology, 12, 564-574.
GOODLETT, C., COROUGE, I., JOMIER, M. & GERIG, G. (2005) A quantitative DTI fiber tract analysis suite, in MICCAI Workshop on open source software. Palm Springs, CA USA.
HALABIEH, O. & WAN, J. (2008) Simulating mechanism of brain injury during closed head impact. Biomedical Simulation, 3, 107-118.
HOLMIN, S., S'DERLUND, J., BIBERFELD, P. & MATHIESEN, T. (1998) Intracerebral inflammation after human brain contusion. Neurosurgery, 42, 291-298
HOLZAPFEL, G. A., GASSER, T. C. & OGDEN, R. W. (2000) A new constitutive framework for arterial wall mechanics and a comparative study of material models. Journal of elasticity, 61, 1-48.
HORGAN, T. J. & GILCHRIST, M. D. (2003) The creation of three-dimensional finite lement models for simulating head impact biomechanics. International Journal of Crashworthiness, 8, 353-366.
HORGAN, T. J. & GILCHRIST, M. D. (2004) Influence of FE model variability in predicting brain motion and intracranial pressure changes in head impact simulations. International Journal of Crashworthiness, 9, 401-418.
HRAPKO, M., VAN DOMMELEN, J. A. W., PETERS, G. W. M. & WISMANS, J. (2008) The influence of test conditions on characterization of the mechanical properties of brain tissue. Journal of Biomechanical Engineering, 130, 31-38.
HURLEY, R. A., MCGOWAN, J. C., ARFANAKIS, K. & TABER, K. H. (2004) Traumatic axonal injury: novel insights into evolution and identification. Journal of Neuropsychiatry and Clinical Neurosciences, 16, 1-17.
JOHNSON, E. A. C. & YOUNG, P. G. (2005) On the use of a patient-specific rapid-prototyped model to simulate the response of the human head to impact and comparison with analytical and finite element models. Journal of Biomechanics, 38, 39-51.
KLEIVEN, S. (2002) Finite element modeling of the human Head. Depart-

ment of Aeronautics, Royal Institute of Technology, Stockholm, Sweden.
KLEIVEN, S. & HOLST, H. V. (2002) Consequences of head size following trauma to the human head. Journal of Biomechanics, 35, 153-160.
LANGLOIS, J. A., RUTLAND-BROWN, W. & THOMAS, K. E. (2004) Traumatic brain injury in the United States: emergency department visits, hospitalizations, and deaths. Atlanta, GA: Centers for Disease Control and Prevention, National Center for Injury Prevention and Control, 1-68.
MATLAB version 6.5.1. Natick, Massachusetts: The MathWorks Inc., 2003.
MARGULIES, S. S. & THIBAULT, L. E. (1992) A proposed tolerance criterion for diffuse axonal injury in man. Journal of Biomechanics, 25, 917-923.
MENDIS, K. K., STALNAKER, R. L. & ADVANI, S. H. (1995) A constitutive relationship for large deformation finite element modeling of brain tissue. Journal of Biomechanical Engineering, 117, 279-286.
MILLER, K. & CHINZEI, K. (1997) Constitutive modelling of brain tissue: experiment and theory. Journal of Biomechanics, 30,1115-1121.
MORI, S., CRAIN, B. J., CHACKO, V. P. & VAN ZIJL, P. C. M. (1999) Three-dimensional tracking of axonal projections in the brain by magnetic resonance imaging. Annals of Neurology, 45, 265-269.
MORI, S., KAUFMANN, W. E., DAVATZIKOS, C., STIELTJES, B., AMODEI, L., FREDERICKSEN, K., PEARLSON, G. D., MELHEM, E. R., SOLAIYAPPAN, M., RAYMOND, G. V., MOSER, H. W. & ZIJL, P. C. M. V. (2002) Imaging cortical association tracts in the human brain using diffusion-tensor-based axonal tracking. Magnetic Resonance in Medicine, 47, 215-223.
MULLER, R. & RUEGSEGGER, P. (1995) Three-dimensional finite element modelling of non-invasively assessed trabecular bone structures. Medical Engineering and Physics, 17, 126-133.
NING, X., ZHU, Q., LANIR, Y. & MARGULIES, S. S. (2006) A transversely isotropic viscoelastic constitutive equation for brainstem undergoing finite deformation. Journal of biomechanical engineering, 128, 925-933.
OZTURK, A., SASSON, A. D., FARRELL, J. A. D., LANDMAN, B. A., DA MOTTA, A. C. B. S., ARALASMAK, A. & YOUSEM, D. M. (2008) Regional Differences in Diffusion Tensor Imaging Measurements: Assessment of Intrarater and Interrater Variability. AJNR Am J Neuroradiol, 29, 1124-1127.
PARIZEL, P. M., ZSARLAK, ., VAN GOETHEM, J. W., VAN DEN HAUWE, L., DILLEN, C., VERLOOY, J., COSYNS, P. & DE SCHEPPER, A. M. (1998) Imaging findings in diffuse axonal injury after closed head trauma. European Radiology, 8, 960-965.

PRANGE, M. T. & MARGULIES, S. S. (2002) Regional, directional, and age-dependent properties of the brain undergoing large deformation. Journal of Biomechanical Engineering, 124, 244-252.
RUAN, J. S., KHALIL, T. & KING, A. I. (1991) Human Head Dynamic Response to Side Impact by Finite Element Modeling. Journal of Biomechanical Engineering, 113, 276-283.
RUAN, J. S., KHALIL, T. & KING, A. I. (1994) Dynamic response of the human head to impact by three-dimensional finite element analysis. Journal of Biomechanical Engineering, 116, 44-50.
RUAN, J. S., KHALIL, T. B. & KING, A. I. (1993) Finite element modeling of direct head impact. 37th Stapp Car Crash Conference Proceedings. SAE International.
SMITH, D. & MEANEY, D. (2000) Axonal damage in traumatic brain injury. The Neuroscientist, 6, 483-495
SORENSON, S. B. & KRAUS, J. F. (1991) Occurrence, severity, and outcomes of brain injury. The Journal of Head Trauma Rehabilitation, 6, 1-10
TUCH, D. S., REESE, T. G., WIEGELL, M. R., MAKRIS, N., BELLIVEAU, J. W. & WEDEEN, V. J. (2002) High angular resolution diffusion imaging reveals intravoxel white matter fiber heterogeneity. Magnetic Resonance in Medicine, 48, 577-582.
VAN DOMMELEN, J. A. W., HRAPKO, M. & PETERS, G. W. M. (2008) Mechanical properties of brain tissue: Characterisation and constitutive Modelling. Mechanosensitivity of the Nervous System. A. Kamkin and I. Kiseleva (eds.) Springer, 249-279.
WILLIAMS, A. J., HARTINGS, J. A., LU, X. C. M., ROLLI, M. L. & TORTELLA, F. C. (2006) Penetrating ballistic-like brain injury in the rat: differential time courses of hemorrhage, cell death, inflammation, and remote degeneration. Journal of Neurotrauma, 23, 1828-1846.
WILLINGER, R. & BAUMGARTNER, D. (2003) Human head tolerance limits to specific injury mechanisms. International Journal of Crashworthiness, 8, 605-618.
ZHANG, H., YUSHKEVICH, P. A., ALEXANDER, D. C. and GEE, J. C. (2006) Deformable registration of diffusion tensor MR images with explicit orientation optimization. Medical Iimage Analysis. 10, 764-785.